

Supporting Information

Simple, Fast, and Precise Counting of Viable Bacteria by Resazurin-Amplified Picoarray Detection

Kuangwen Hsieh,[§] Helena C. Zec,[‡] Liben Chen,[§] Aniruddha Kaushik,[§] Kathleen E. Mach,[†] Joseph C. Liao,[†] Tza-Huei Wang^{*,§,‡}

[§]Department of Mechanical Engineering, Johns Hopkins University, Baltimore, Maryland 21218, United States

[‡]Department of Biomedical Engineering, Johns Hopkins School of Medicine, Baltimore, Maryland 21205, United States

[†]Department of Urology, Stanford University School of Medicine, Stanford, California 94305, United States

* To whom correspondence should be addressed; E-mail: thwang@jhu.edu; Phone: (+1) 410-516-7086.

The Supporting Information document for this work includes Experimental Section (Bacteria Stock and Storage, Photomask Design and Printing, Master Mold Microfabrication, Picoarray Device Fabrication, Bacterial Sample Preparation, Measurement of Bacterial Sample Concentrations via Plating, Sample Loading and Digitization, Stochastic Confinement of Single Bacteria in Picochambers, Incubation and Fluorescence Detection, Image and Data Analysis, and Derivation of Equation (1) to Calculate Bacteria Counts), Supplementary Figures (Picoarray Operation by Untrained Off-Site User, Validation of Resazurin-Amplified Fluorescence Detection, Confirmation of Increasing Fluorescence in Picochambers, Sample Evaporation within Picochambers from Incubation, Triplicated Quantification of *E. coli* Samples at the Same Concentration, Measurement of *E. coli* Stock Concentration via Plating, Quantitative Analysis in Multi-RAPiD for *E. coli*, Coefficients of Variation from Plating and RAPiD for *E. coli*, Measurement of *S. aureus* Stock Concentration via Plating, Quantitative Analysis in Multi-RAPiD for *S. aureus*, and Coefficients of Variation from Plating and RAPiD for *S. aureus*), and descriptions of Supplementary Videos (Sample Loading in Picoarray and Sample Digitization in Picoarray).

Experimental Section

Bacteria Stock and Storage

Reference strains of *E. coli* (ATCC 25922, ATCC, Manassas, VA) and *S. aureus* (ATCC 29213, ATCC, Manassas, VA) were separately plated on tryptic soy agar plates (TSA; BD Difco™, Becton, Dickinson and Company, Franklin Lakes, NJ) at 37 °C overnight. Several isolated colonies from each plate were grown in tryptic soy broth (TSB; BD Bacto™, Becton, Dickinson and Company, Franklin Lakes, NJ) at 37 °C to log phase. Both bacterial stocks in TSB were then supplemented with sterile glycerol (E520, AMRESCO, Solon, OH) at 20% v/v, aliquoted, and frozen at -80 °C until use. After the aliquoted stocks were completely frozen, one aliquot for each strain was thawed and counted via plating in one TSA plate, which accounts the potential effect of adding glycerol and freezing bacteria and thus provides a more accurate initial estimate of the stock concentrations.

Photomask Design and Printing

The simplicity of the Picoarray device allowed us to use only a cost-effective transparency photomask toward device fabrication. The photomask was designed in L-Edit v16.0 (Tanner EDA, Monrovia, CA) and printed onto a high-quality transparency at 20000 dpi by CAD/Art Services, Inc. (Bandon, OR). The transparency mask was taped on a five-inch soda lime glass mask holder (HTA Enterprises, San Jose, CA) and stored in cleanroom environment prior to use.

Master Mold Microfabrication

Only an alignment-free, single-step, standard SU8 photolithography process was required for microfabricating the master molds that were used to cast PDMS fluidic layers toward device fabrication. Briefly, four-inch silicon wafers (Polishing Corporation of America, Santa Clara, CA) were first dehydration baked at 200 °C for at least 2 h. Next, a ~50- μ m-thick layer of SU8-3025 (MicroChem Corp., Newton, MA) was spin coated onto each silicon wafer at 2300 rpm for 30 s, soft baked at 95 °C for 40 min, exposed and patterned at 250 mJ/cm² with a contact aligner, post-exposure baked at 95 °C for 5 min, and developed in SU8 developer (MicroChem Corp., Newton, MA) for ~10 min to generate the patterns of fluidic channels, connecting channels, and picochambers. Patterned SU8-3025 was finally hard baked at 200 °C for 1 h to complete microfabrication. All master molds used in this work were stored in cleanroom environment.

Picoarray Device Fabrication

The Picoarray device was fabricated by assembling three modular layers – the PDMS fluidic layer, the PDMS cover layer, and the glass layer. The PDMS fluidic layer contains all fluidic features of the device, including inlets, outlets, branch channels, connecting channels, and picochambers. The PDMS cover layer is a ~100- μ m-thick layer that is sandwiched between the PDMS fluidic layer and the glass layer, which covers the glass and renders PDMS as the only surface material inside the device.

The PDMS fluidic layer was fabricated using the standard soft lithography technique using SYLGARD 184 Silicone Elastomer Kits (Dow Corning, Midland, MI). Master molds for the fluidic layers were treated with chlorotrimethylsilane (92361, Sigma-Aldrich, St. Louis, MO) via vapor deposition in a vacuum chamber for ~5 min, which serves to minimize adhesion of PDMS to the master molds. Approximately 40 g of 10:1 (w/w) PDMS was poured onto the fluidic layer molds, covering all features on the fluidic layer mold with a 3 – 4-mm-thick layer of PDMS. PDMS was vacuumed for ~20 min to remove air bubbles and baked at 80 °C for ~25 min. Cured PDMS fluidic layers were removed from the master molds and cut into individual chips. Fluidic access holes were punched into individual

chips with sharpened needles (20 gauge; McMaster-Carr, Elmhurst, IL). The fluidic layer chips could be used immediately or stored in cleanroom environment for later use.

The PDMS cover layer was fabricated by transferring the thin PDMS layer from a blank wafer to the glass bottom layer using a PDMS sacrificial layer. We used this fabrication process because spin-coating PDMS directly on the glass layer resulted in thicker PDMS at the corners of the glass layer, which caused uneven bonding with the PDMS fluidic layer and leaky devices. In this fabrication process, 15:1 (w/w) PDMS was spun onto a blank silicon wafer and baked at 80 °C for ~4 min to form the thin PDMS cover layer. In addition, 6:1 (w/w) PDMS was spun onto a separate blank silicon wafer and baked at 80 °C for ~5 min to form the sacrificial layer (~1 mm in thickness). The sacrificial layer was peeled from its blank wafer and placed directly on the PDMS cover layer, which remained on its blank wafer. The attached layers were baked at 80 °C for ~5 min and thermally-enhanced adhesion allowed the two layers to be peeled from the blank wafer without separation. The thermally-bonded layers were cut to the same dimensions as the fluidic layer chips, and could be used immediately or stored in cleanroom environment for later use. The exposed surface of the PDMS cover layer and a cover glass (43 mm × 50 mm, thickness = ~0.19 to 0.25 mm; Ted Pella, Inc., Redding, CA) were then treated with O₂ plasma (45 s, 30 W, 500 mTorr), brought into contact, and immediately baked for at 80 °C ~5 min. As the PDMS cover layer became firmly bonded to the cover glass, the sacrificial layer could be peeled from the PDMS cover layer without damages.

To complete device fabrication, the exposed surface of the PDMS cover layer and a PDMS fluidic layer were treated with O₂ plasma (45 s, 30 W, 500 mTorr), brought into contact, and immediately baked for at 80 °C ~5 min. All Picoarray devices were stored at 80 °C for at least 24 hours before use. Finally, prior to experimentation, inlets and outlets of devices were covered with Scotch tape, and devices were placed in a vacuum chamber for > 2 h.

Bacterial Sample Preparation

Aliquots of bacteria stock were thawed in a 37 °C water bath (Isotemp, Thermo Fisher Scientific, Waltham, MA) for ~5 min and immediately washed twice with BD BBL™ Mueller Hinton II broth (cation-adjusted) (297963, Becton, Dickinson and Company, Franklin Lakes, NJ). For each wash, each aliquot of bacteria was centrifuged (5418R, Eppendorf, Germany) at 10000 rpm for 5 min, and the supernatant was removed before the bacteria pellet was resuspended in fresh Mueller-Hinton broth and mixed via pipetting and gentle vortex. Washed bacteria stock was subsequently diluted with Mueller-Hinton broth to 2.5× concentrated stocks. Each final sample was composed of 40% bacteria stock, 50% Mueller-Hinton broth, and 10% AlamarBlue (DAL1025, Thermo Fisher Scientific, Waltham, MA). All bacterial samples were prepared and used immediately in experiments.

Measurement of Bacterial Sample Concentrations via Plating

All *E. coli* and *S. aureus* samples, follow sample wash, were titrated with Mueller-Hinton broth down to 5.0×10^2 , 2.5×10^2 , 1.25×10^2 CFU/mL. Two-hundred μL from each of the 3 titrations was plated in a TSA plate, resulting in three plates with expected CFU counts of 100, 50, and 25, respectively. All TSA plates were incubated at 37 °C, though plates with *E. coli* were incubated for 12 h, whereas plates with *S. aureus* were incubated for 24 h. After incubation, the number of colonies on each plate was manually counted and recorded directly on the plate. Each measurement was repeated for 3 separate samples, resulting in a total of 9 data points (*i.e.*, 3 titrations in triplicate). The counted number of colonies was plotted against the expected number of colonies, and a linear fit was performed. The linearity was examined and the slope was calculated. Finally, if necessary, the slope of the linear fit line was used to recalculate the bacterial sample concentration.

Sample Loading and Digitization

In this work, samples can be efficiently loaded into the device and digitized within picochambers via vacuum-assisted sample loading and oil-driven sample digitization. Prior to removing the devices from the vacuum chamber, all samples were drawn into the plastic housings of separate blunt-end needles with empty 1-mL syringes. Pre-filling samples in the de facto sample holders minimized the time that devices were kept at atmosphere and losing negative pressure. Once the devices were removed from the vacuum chamber, blunt-end needles were then sequentially inserted through the Scotch tape and into device inlets. Notably, keeping the syringes attached to the needles and the needles plugged in the device have been empirically determined to ensure robust vacuum-assisted sample loading. To ensure that all picochambers were filled with samples, the sample-containing blunt-end needles were kept in the device for 2 – 3 min before they were removed from the inlets. Blunt-end needles and Tygon tubings that carried 100 cSt silicone oil (378364, Sigma-Aldrich, St. Louis, MO) were then inserted into device inlets. The oil tubings were connected via manifolds to a pressure regulator. The Scotch tape covering the device outlets were removed and 10 psi was applied to drive the silicone oil through the branch channels of the device. Silicone oil typically flowed evenly through the multiple units and out of the device outlets in < 1 min. Once silicone oil completely displaced the samples and flowed out the device outlets, the pressure was decreased to 1 psi and epoxy-filled blunt-end needles were inserted into device outlets to function as sealing plugs for the device.

Food dyes (Ateco, Glen Cove, NY) were used as mock samples for visualizing and acquiring videos and pictures of vacuum-assisted sample loading and oil-driven sample digitization. Videos and micrographs were acquired under an inverted microscope (IX71; Olympus Corp., Tokyo, Japan) with a digital single-lens reflex (DSLR) camera (EOS 60D; Canon, Inc., Tokyo, Japan). Videos were trimmed and annotated in Microsoft Movie Maker. Dusts on the outside surfaces of the devices, which did not affect sample loading or sample digitization were digitally removed from the images for aesthetics via Adobe Photoshop. The tone and the contrast of the images were also enhanced via Adobe Photoshop.

For additional demonstration of the user-friendliness of Picoarray and its operation, several Picoarray devices were shipped to Stanford University School of Medicine, where a collaborator with no microfluidic expertise or prior experience with Picoarray replicated vacuum-assisted sample loading and oil-driven sample digitization using a food dye as mock sample. At Stanford University, oil-driven sample digitization was achieved by pumping 100 cSt silicone oil with a syringe pump (NE-1000, New Era Pump Systems Inc., Farmingdale, NY) at 15 $\mu\text{L}/\text{min}$ instead of using pressure. Photographs were acquired with an iPhone 5 camera. Micrographs were acquired under an inverted microscope (AxioObserver A1, Zeiss, Germany) with a CCD camera (AxioCam MRc, Zeiss, Germany) Again, dusts and fibers on the outside surfaces of the devices, which did not affect sample loading or sample digitization, were digitally removed from the images for aesthetics via Adobe Photoshop. The tone and the contrast of the images were also enhanced via Adobe Photoshop.

Stochastic Confinement of Single Bacteria in Picochambers

Stochastic confinement of bacteria in picochambers is a Poisson process. The probability of finding x bacteria in a picochamber is given by

$$P(x) = \frac{\lambda^x}{x!} e^{-\lambda} \quad (\text{S-1}),$$

where λ is the average number of bacteria per picochamber, as determined by product of the input concentration of bacteria and the picochamber volume. As an example, in part of this work, $\lambda = 0.2$ was chosen to ensure that single-cell encapsulated picochambers could be frequently observed under

fluorescence microscopy, while minimizing the encapsulation of 2 or more cells in a picochamber. In our Picoarray with 250-pL picochambers, $\lambda = 0.2$ was achieved at 8×10^5 CFU/mL bacterial input concentration.

Incubation and Fluorescence Detection

The device was placed on a flat-bed PCR machine (ProFlex™ 2× flat PCR System, Thermo Fisher Scientific, Waltham, MA), which was kept at 37 °C for the entire incubation period except for measuring the fluorescence intensities within the picochamber array, during which the device was imaged with a fluorescence microscope (BX51, Olympus, Japan). The fluorescence microscope is equipped with a mercury lamp, an AlamarBlue-compatible filter cube (49305; Chroma Technology Corp., Bellows Falls, VT), a 1.25× magnification objective lens (Olympus PlanAPO N 1.25×/0.04 NA), and a digital CCD camera (Retiga EXi Fast 1394, QImaging, Canada). The filter cube has a 546/22 nm excitation filter, a 565 nm dichroic beamsplitter, and a 590/33 nm emission filter. The CCD camera is connected to a PC and interfaced with QCapture software (QImaging, Canada). For each fluorescence image acquisition, the mercury lamp was warmed for ~5 min before the device was moved from the flat-bed PCR machine to the fluorescence microscope. The shutter was manually switched on, a 12-bit image was immediately acquired under 500-ms exposure, and the shutter was immediately manually switched off. This acquisition process was performed for each unit of the device.

Image and Data Analysis

Data acquisition from fluorescence images and subsequent data analysis were performed using ImageJ (1.48v), Microsoft Excel 2010, and Origin 8.0. Fluorescence intensities in the picochambers and background fluorescence were measured with ImageJ. Downstream data analyses were performed in Microsoft Excel 2010 and Origin 8.0. For example, data sorting based on the position in the picochamber array and the fluorescence intensities, data normalization, and histogram analysis were performed in Excel. Thresholding negative from positive picochambers was calculated via Origin. Moreover, all plots in this work were plotted with Origin.

Fluorescence images were first rotated (if necessary), cropped around the 600 picochambers in the observation area, and applied with an orange pseudo-color in ImageJ. Using the “Threshold” function in ImageJ, a lower threshold value for each image was set such that all 600 picochambers were selected for analysis. Because the background is darker than the picochambers, the “Dark Background” option was selected. Subsequently, the area, mean gray value (*i.e.*, mean fluorescence intensity), minimum and maximum gray values (*i.e.*, minimum and maximum fluorescence intensities), and center of mass (with X and Y coordinates) of each picochamber was individually measured using the “Analyze Particles” function. For each fluorescence image, a vertical line and a horizontal line were drawn at the center of the image and outside of picochambers, and background fluorescence values were measured from these center lines using the “Measure” function. These measurement data were exported to Microsoft Excel for downstream analysis. Of note, strong fluorescence of AlamarBlue and high contrast between the strongly fluorescent picochambers and weakly fluorescent branch channels facilitated this analysis workflow.

All data sets measured via ImageJ were subsequently analyzed with Excel and Origin. Picochamber measurement data were first imported in Excel and sorted based on the X and Y coordinates such that the gray values (*i.e.*, fluorescence intensities) were rearranged based on the appropriate columns and rows in the picochamber array, where the top left picochamber of each image was designated as picochamber 1 and the bottom right picochamber was designated as picochamber 600. The background fluorescence of each image was calculated as length-based weighted average of the line

measurements of the vertical line and the horizontal line. For each condition, background-normalized fluorescence signals at 3 h were plotted into a histogram by using the “Histogram” function in Excel. The histogram data were subsequently plotted in Origin as a scatter plot, which allowed for fitting a single Gaussian peak around the negative picochamber population and computation of the mean (x_c) and the sigma (σ) of the fitted Gaussian peak via the “Fit Single Peak” function in Origin. In this work, thresholds were set at $x_c + 4 \times \sigma$ to ensure that positive picochambers could be differentiated from negative picochambers with high confidence. Each threshold computed from Origin was then applied to the data sets in Excel to count the number of positive picochambers. Finally, using Equation 1, the number of bacterial cells was calculated from the number of positive picochambers. This correction serves to account picochambers that had trapped multiple bacterial cells.

Following triplicated multi-RAPiD experiments for both *E. coli* and *S. aureus* (*i.e.*, 3 different samples in 3 different Picoarray devices for each species), the mean and the standard deviation from each of the 4 titrations were computed in Excel. Coefficient of variation (CV) at each titration was subsequently calculated by dividing the standard deviation by the mean in Excel, and then plotted against each expected number of positive picochambers in Origin. The calculated numbers of bacterial cells were plotted against both the expected concentrations of the bacterial sample and the expected numbers of positive picochambers in Origin. Using the “Fit Linear” function in Origin, a linear line was fit between the calculated numbers of bacterial cells and the expected numbers of positive picochambers, and the slope and the R^2 of the linear fit line were computed.

Derivation of Equation (1) to Calculate Bacteria Counts

Starting with the Poisson equation (*i.e.*, Equation (S-1)), the probability of finding 0 bacteria in a picochamber (*i.e.*, an empty picochamber) reduces the equation to

$$P(0) = e^{-\lambda} \quad (\text{S-2}).$$

For a large number of picochambers, the fraction of observable empty picochambers can be used as an estimator for $P(0)$; that is

$$P(0) = \frac{\text{Total} - \text{Positive}}{\text{Total}} = e^{-\lambda} \quad (\text{S-3}).$$

Solving for λ gives

$$\lambda = -\ln\left(\frac{\text{Total} - \text{Positive}}{\text{Total}}\right) \quad (\text{S-4}).$$

Because λ is the average number of bacteria per picochamber, Equation (S-4) becomes

$$\frac{\text{Bacteria}}{\text{Total}} = -\ln\left(\frac{\text{Total} - \text{Positive}}{\text{Total}}\right) \quad (\text{S-5}).$$

Finally, rearranging Equation (S-5) gives

$$\text{Bacteria} = -\ln\left(\frac{\text{Total} - \text{Positive}}{\text{Total}}\right) \times \text{Total} \quad (1).$$

Supplementary Figures

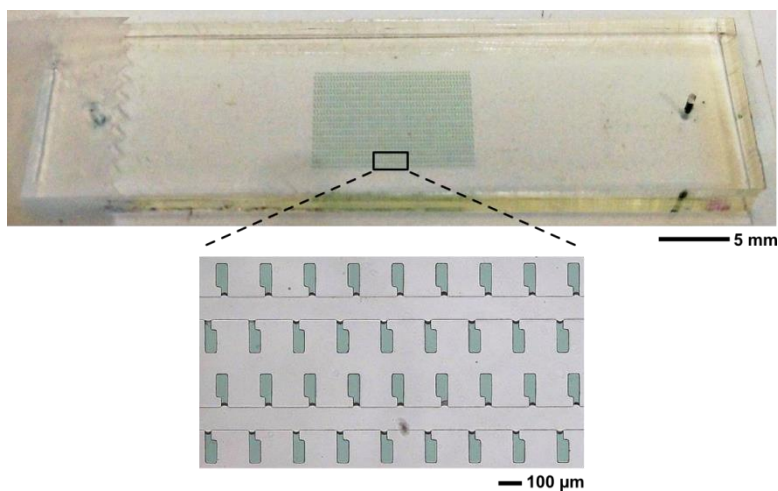
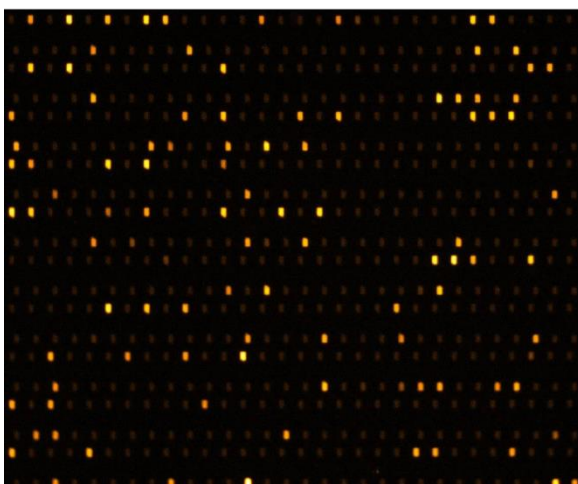


Figure S-1. Picoarray Operation by Untrained Off-Site User. The user-friendliness of Picoarray and its operation allows easy adoption by untrained users. As a demonstration, several Picoarray devices are shipped to Stanford University School of Medicine, where a collaborator with no microfluidic expertise or prior experience with Picoarray is asked to perform vacuum-assisted sample loading and oil-driven sample digitization. After walking through the experimental procedures only via video conferencing, the collaborator successfully replicates the procedures (**top** photograph) with complete digitization of picochambers (**bottom** micrograph). These results clearly demonstrate the robustness, reproducibility, and accessibility of Picoarray and its operation.

Resazurin-Amplified Fluorescence Detection



Bright Field Detection (*i.e.*, No Resazurin-Amplification)

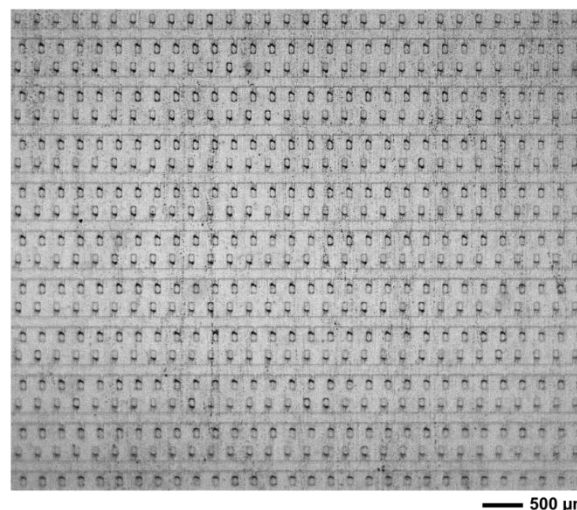


Figure S-2. Validation of Resazurin-Amplified Fluorescence Detection. To validate the importance of resazurin-amplified fluorescence for detecting bacteria in picochambers, a sample with 8×10^5 CFU/mL *E.coli*, Mueller-Hinton broth, and AlamarBlue (a resazurin-based fluorescent dye) is loaded into a Picoarray device. At this sample concentration, ~20% picochambers are expected to confine single *E.coli*. After 37 °C incubation for 3 h, the array is detected with either wide-field fluorescence microscopy (**left**) or wide-field bright-field microscopy (**right**). Under fluorescence microscopy, ~20% randomly-located picochambers with strong fluorescence are indeed observed within the observation area, which matches the expectation and strongly supports that single *E.coli* are stochastically confined in picochambers in accordance to Poisson distribution. In contrast, when observing the same array under bright field, picochambers with or without *E.coli* cannot be differentiated. These results strongly signify the importance of using resazurin-amplified fluorescence for detecting bacteria in picochambers.

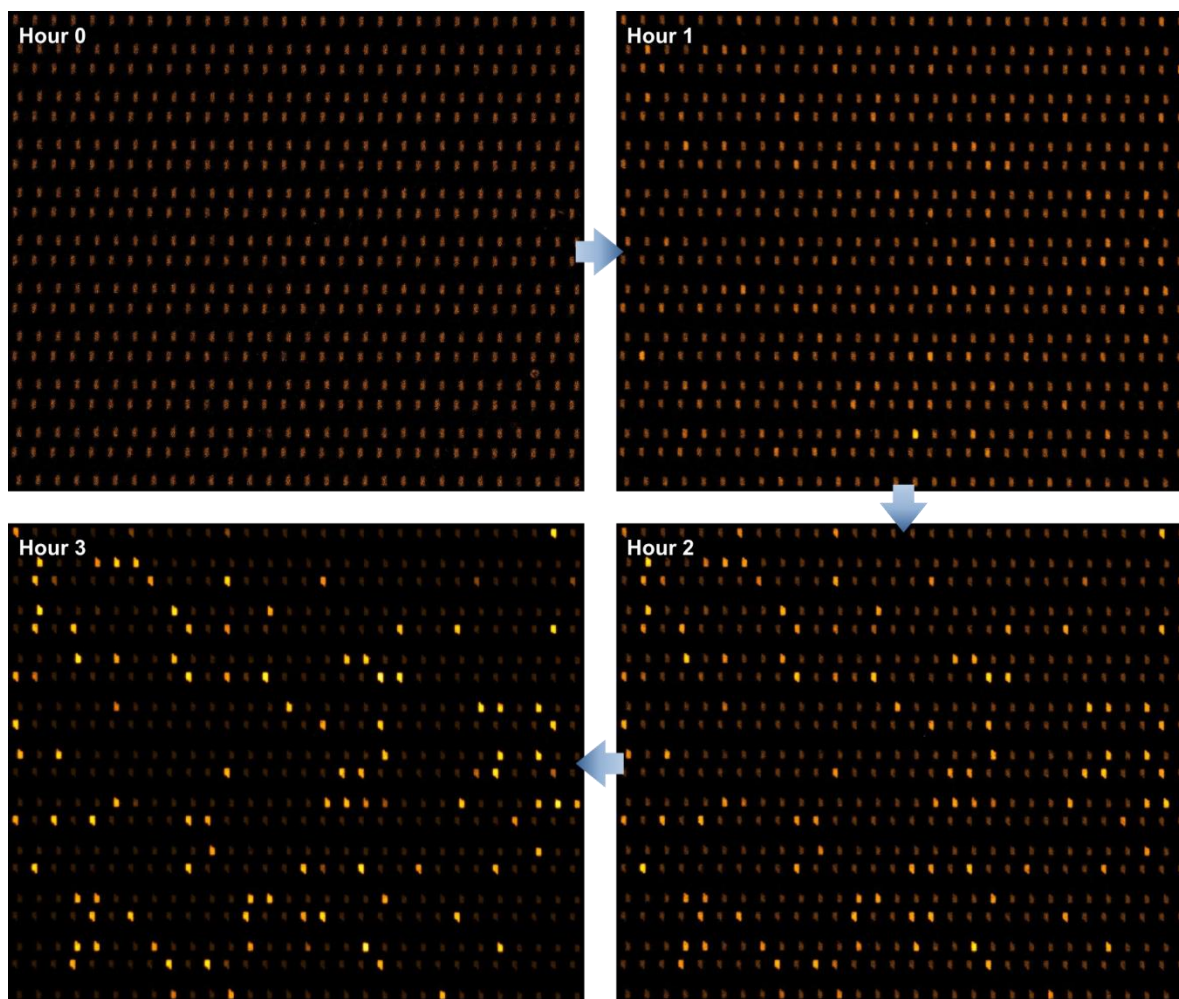


Figure S-3. Confirmation of Increasing Fluorescence in Picochambers. To verify that bacteria are isolated in picochambers and replicating, a sample with 8×10^5 CFU/mL *E.coli*, Mueller-Hinton broth, and AlamarBlue is loaded into a Picoarray device, incubated at 37 °C, and the fluorescence intensity of 600 picochambers is tracked via wide-field fluorescence microscopy at 1 h interval for 3 h. At this sample concentration, ~20% picochambers are expected to trap single *E.coli* and yield fluorescence (*i.e.*, positive picochambers). Initially at 0 h (**top left**), only background fluorescence can be observed in all picochambers. After 1 h (**top right**), fluorescence can be detected in several picochambers. Increased fluorescence intensity can be observed in ~20% randomly-located picochambers after 2 h (**bottom right**), which is on par with the expected number of positive picochambers. Finally, strong fluorescence can be detected from the same picochambers after 3 h (**bottom left**). These results strongly suggest that *E. coli* cells are isolated in those picochambers and have been replicating and generating fluorescence.

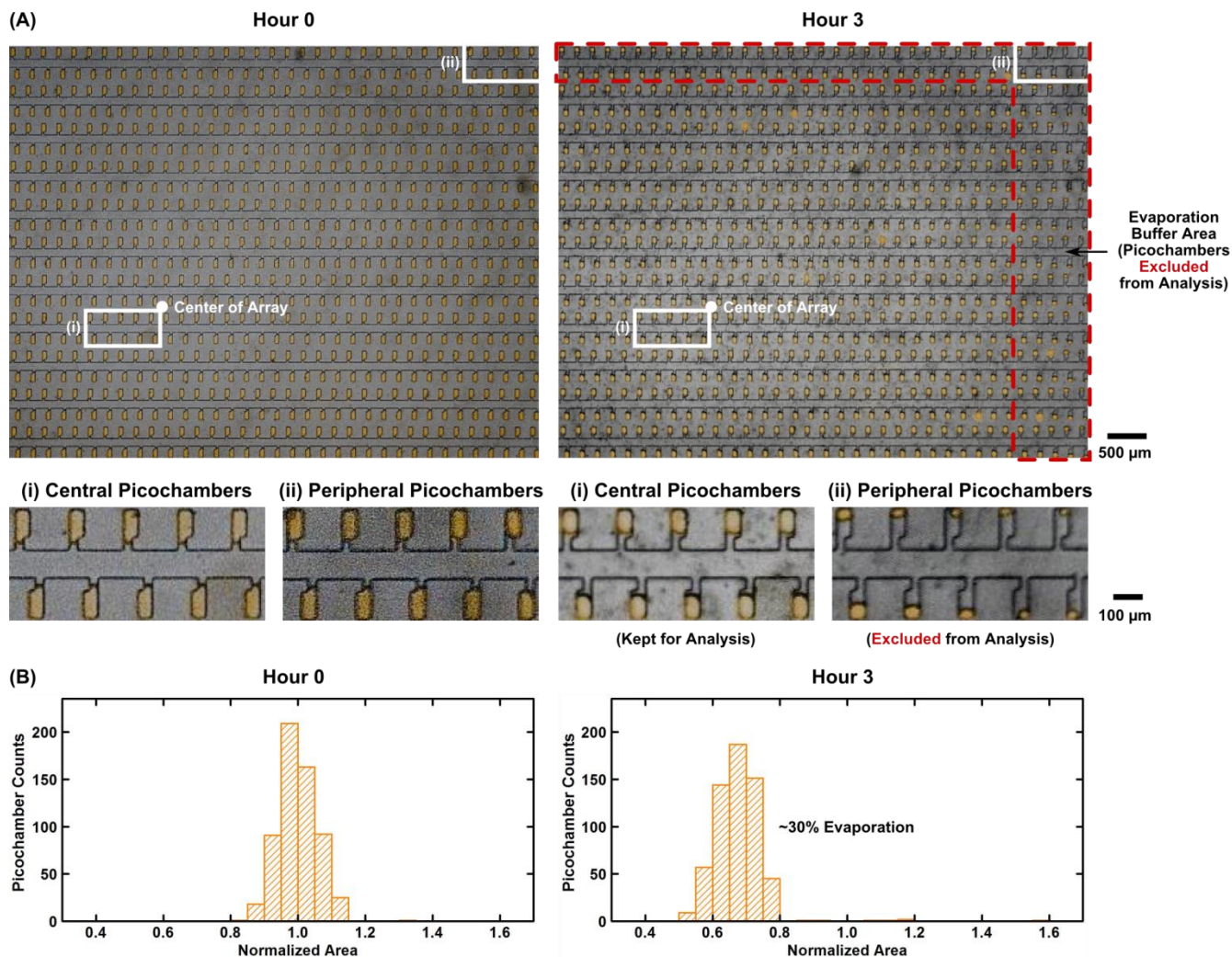


Figure S-4. Sample Evaporation within Picochambers from Incubation. (A) Micrographs of the same sample-filled array unit within a Picoarray device clearly show reductions in sample volumes within picochambers across the entire array unit after 3 h incubation at 37 °C, suggesting that samples (pseudocolored for visualization) within picochambers have evaporated during incubation. After 3 h incubation, compared to the (i) central picochambers that are located near the center of the array (white dot), the (ii) peripheral picochambers that are located in the periphery of the array (*e.g.*, toward the top side and the right-hand side) experience more significant evaporation. As such, picochambers from the top branch channel and the first five columns of each branch channel on the right-hand side are used as an “evaporation buffer” area and excluded from analysis. (B) As an estimate of the extend of sample evaporation with picochambers, the area within each picochamber occupied by the sample at both 0 h and 3 h is first calculated from the micrographs using ImageJ. For this calculation, picochambers in the evaporation buffer area are excluded. Each sample area within the picochamber is subsequently normalized to the mean sample area at 0 h. Histograms of normalized sample areas at 0 h and at 3 h indicate that ~30% of the sample evaporates from 3 h incubation while the distribution of normalized sample areas remains similar between 0 h and 3 h.

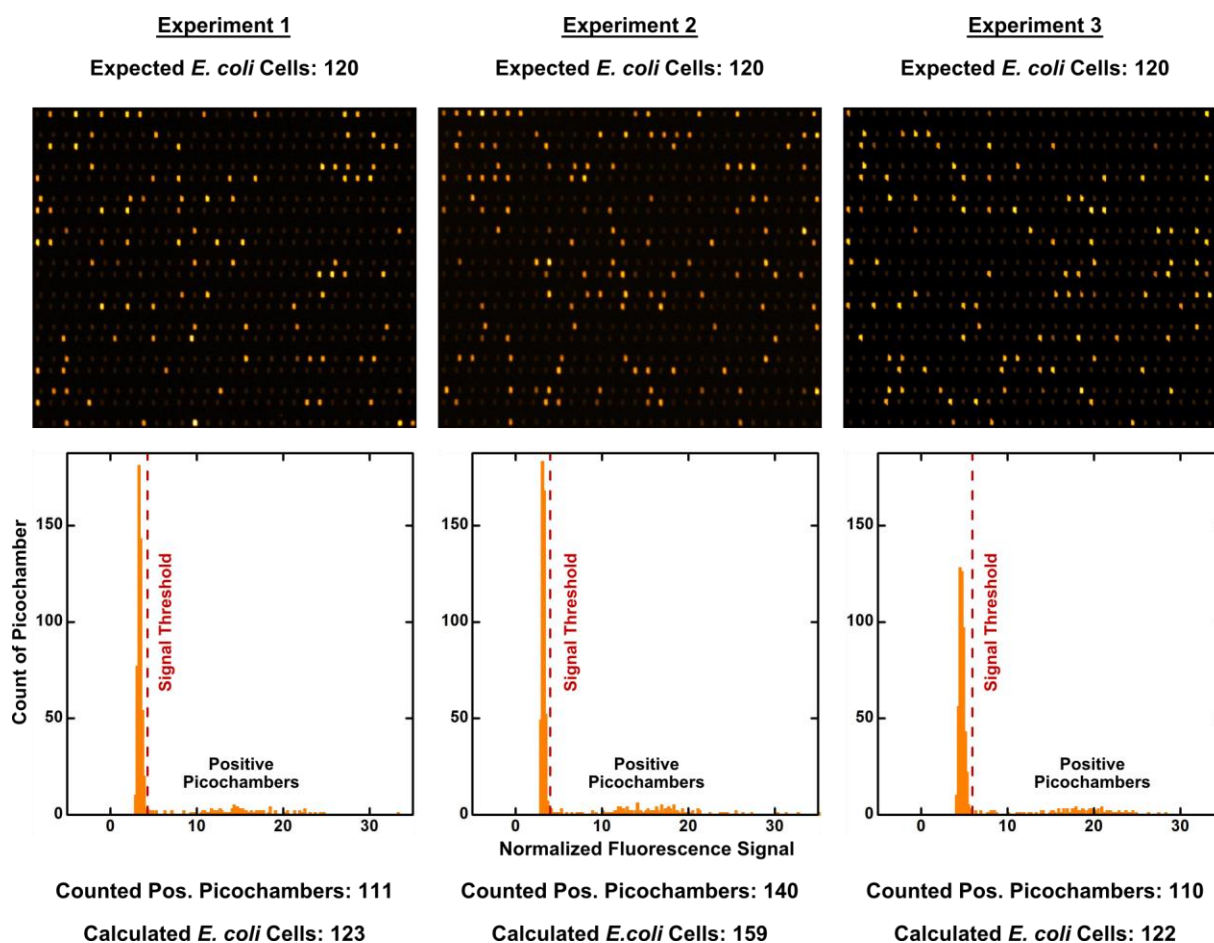


Figure S-5. Triplicated Quantification of *E. coli* Samples at the Same Concentration. Three 8×10^5 CFU/mL *E. coli* samples with Mueller-Hinton broth and AlamarBlue are quantified with three different Picoarray devices in separate experiments. This sample concentration results in a mean occupancy (λ) of 0.2 in our picochamber array, equivalent to approximately 120 picochambers with single *E. coli* and hence with strong fluorescence in an observation area of 600 picochambers. After incubating the device at 37 °C for 3 h, strong fluorescence can be detected in ~20% of the picochambers in each of the three devices. For each of the 3 samples, background-normalized fluorescence signals of 600 picochambers are first plotted in a histogram. Each histogram shows the distribution of a smaller subpopulation of strongly fluorescent picochambers that confined *E. coli* (i.e., positive) and a larger subpopulation of weakly fluorescent empty picochambers. A Gaussian fit for the negative subpopulation of the histograms is performed in Origin. The mean (x_c) and the sigma (σ) are computed from the fitted Gaussian peak of the negative subpopulation. The threshold for differentiating positive picochambers from negative picochambers is set at $x_c + 4 \times \sigma$ (vertical red dash lines). Subsequently, 111, 140, and 110 positive picochambers are counted for the 3 samples, respectively. Correction of the raw counts of positive picochambers (for accounting picochambers that were occupied by multiple *E. coli* cells) increases the number of *E. coli* cells in these 3 samples to 123, 159, and 122, respectively. The mean and standard deviation of the 3 experiments are 134.6 ± 21.5 *E. coli* cells. These results demonstrate the reproducibility of counting single bacterial cells for samples with the same concentration in our Picoarray device.

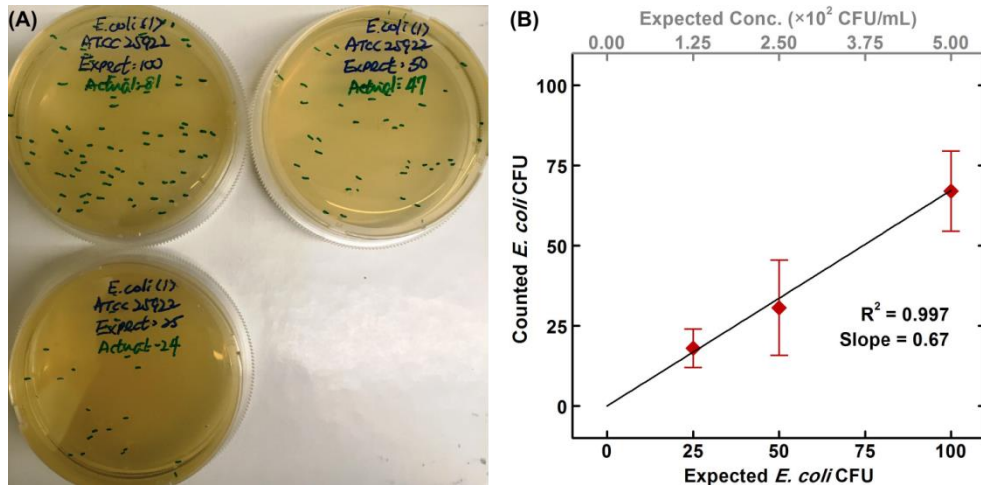


Figure S-6. Measurement of *E. coli* Stock Concentration via Plating. (A) An aliquot of a $\sim 6.0 \times 10^9$ CFU/mL *E. coli* stock (ATCC 25922; originally estimated via a single plate) is divided into 3 titrations (1.25×10^2 , 2.5×10^2 , and 5.0×10^2 CFU/mL), and 200 μ L of each titration is plated in tryptic soy agar plates, resulting in expected CFU counts of 25, 50, and 100, respectively. After 12-h, 37 $^{\circ}$ C incubation, the number of colonies from each titration is manually counted and recorded directly on the plate. (B) After repeating the same experiment for 3 separate aliquots (*i.e.*, 3 titrations in triplicate), the counted number of colonies is plotted against the expected number of colonies. The slope of the linear fit line is 0.67. Consequently, the concentration of this *E. coli* stock is recalculated as 4.0×10^9 CFU/mL. Error bars represent standard deviations from triplicated experiments.

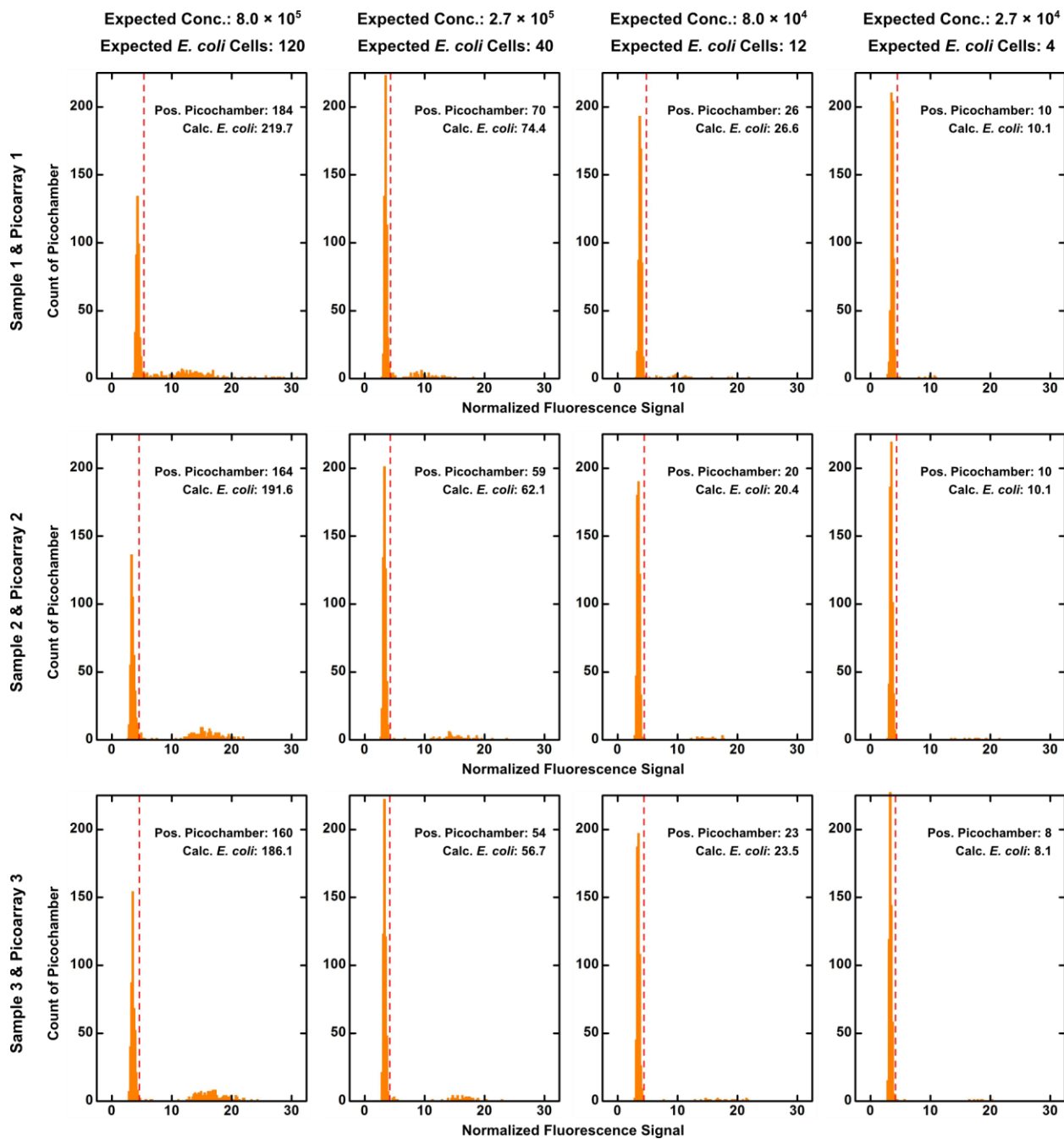


Figure S-7. Quantitative Analysis in Multi-RAPiD for *E. coli*. Three separate *E. coli* samples (estimated at 4.0×10^9 CFU/mL via triplicated plating) are enumerated via multi-RAPiD in 3 independent Picoarray devices. Each *E. coli* sample is titrated to 8.0×10^5 , 2.7×10^5 , 8.0×10^4 , and 2.7×10^4 CFU/mL with Mueller-Hinton broth and AlamarBlue. From these 4 input concentrations, approximately 120, 40, 12, and 4 *E. coli* cells (out of 600 picochambers) are expected to be detected across the 4 array units of each device. Quantitative analysis of each titration is performed by plotting background-normalized fluorescence signals of the 600 picochambers in a histogram, fitting a Gaussian peak around the negative subpopulation of the histogram, which represents the weakly fluorescent empty picochambers, defining the threshold (vertical red dash lines) based on the mean and the sigma of the fitted Gaussian peak, and counting the number of positive picochambers with background-normalized fluorescence signals above the threshold. Finally, the number of positive picochambers is converted to the calculated number of *E. coli* cells to account for picochambers that have entrapped multiple *E. coli* cells.

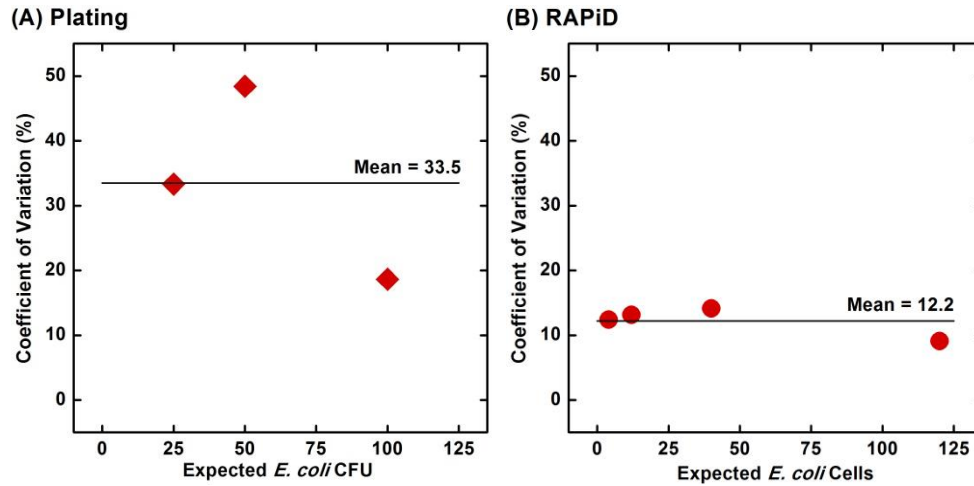


Figure S-8. Coefficients of Variation from Plating and RAPiD for *E. coli*. Coefficients of variation (CV) from enumerating *E. coli* via (A) plating and (B) RAPiD are calculated by dividing the standard deviations by the means at each expected number of *E. coli* CFUs (for plating) or cells (for RAPiD). (A) For plating, at the 3 expected numbers of *E. coli* CFUs, the CVs range from 18.6% to 48.4% and average 33.5% (marked by the horizontal line). (B) In contrast, for RAPiD, at the 4 expected numbers of *E. coli* cells, the CVs range from 9.1% to 14.1% and average at 12.2% (marked by the horizontal line). The smaller spread in CVs from RAPiD provides strong support that RAPiD offers a more precise method for enumerating *E. coli*.

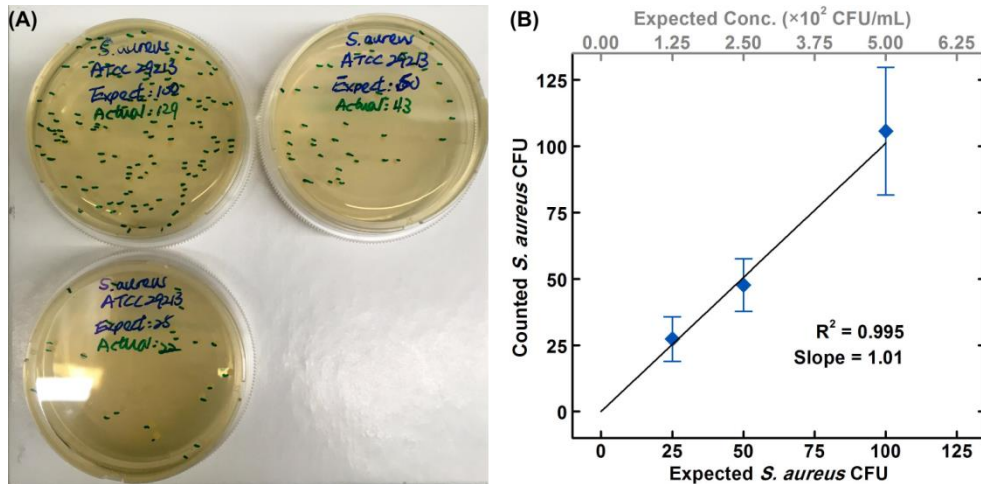


Figure S-9. Measurement of *S. aureus* Stock Concentration via Plating. (A) An aliquot of a $\sim 1.8 \times 10^{10}$ CFU/mL *S. aureus* stock (ATCC 29213; originally estimated via a single plate) is divided into 3 titrations (1.25×10^2 , 2.5×10^2 , and 5.0×10^2 CFU/mL), and 200 μ L of each titration is plated in tryptic soy agar plates, resulting in expected CFU counts of 25, 50, and 100, respectively. After 24-h, 37 $^{\circ}$ C incubation, the number of colonies from each titration is manually counted and recorded directly on the plate. (B) After repeating the experiment for 3 separate aliquots (*i.e.*, 3 titrations in triplicate), the counted number of colonies is plotted against the expected number of colonies. The slope of the linear fit line is 1.01, indicating that the concentration of this *S. aureus* stock is indeed 1.8×10^{10} CFU/mL. Error bars represent standard deviations from triplicated experiments.

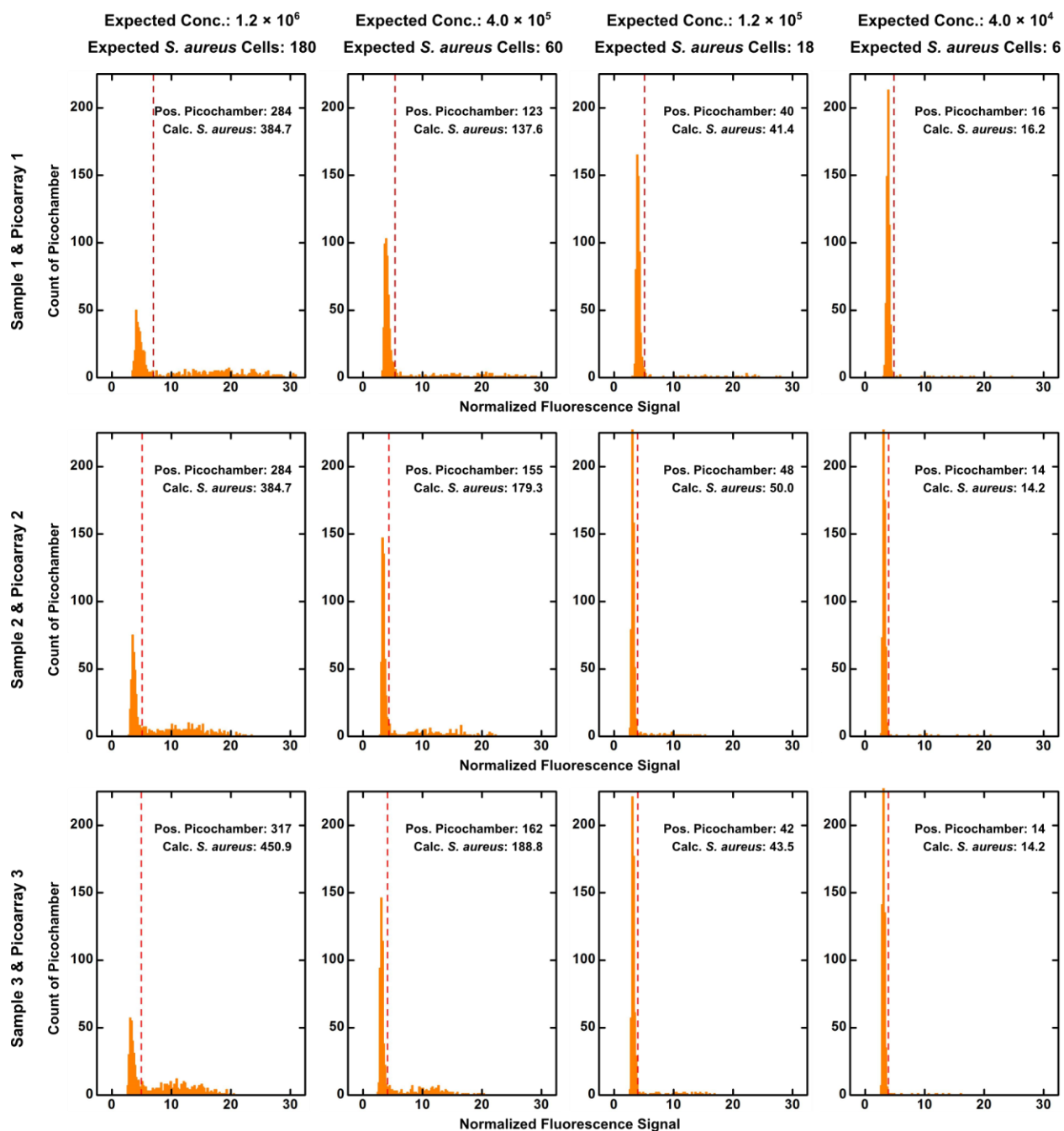


Figure S-10. Quantitative Analysis in Multi-RAPiD for *S. aureus*. Three separate *S. aureus* samples (estimated at 1.8×10^{10} CFU/mL via triplicated plating) are enumerated via multi-RAPiD in 3 independent Picoarray devices. Each *S. aureus* sample is titrated to 1.2×10^6 , 4.0×10^5 , 1.2×10^5 , and 4.0×10^4 CFU/mL with Mueller-Hinton broth and AlamarBlue. From these 4 input concentrations, approximately 180, 60, 18, and 6 *S. aureus* cells (out of 600 picochambers) are expected to be detected across the 4 array units of each device. Quantitative analysis in multi-RAPiD for *S. aureus* proceeds similarly as that for *E. coli*. For each *S. aureus* titration, a histogram is plotted, a Gaussian peak is fitted around the negative subpopulation of the histogram, a threshold is defined (vertical red dash lines), positive picochambers with background-normalized fluorescence signals above the threshold are counted, and finally, the number of *S. aureus* cells is calculated to account for picochambers that have entrapped multiple *S. aureus* cells.

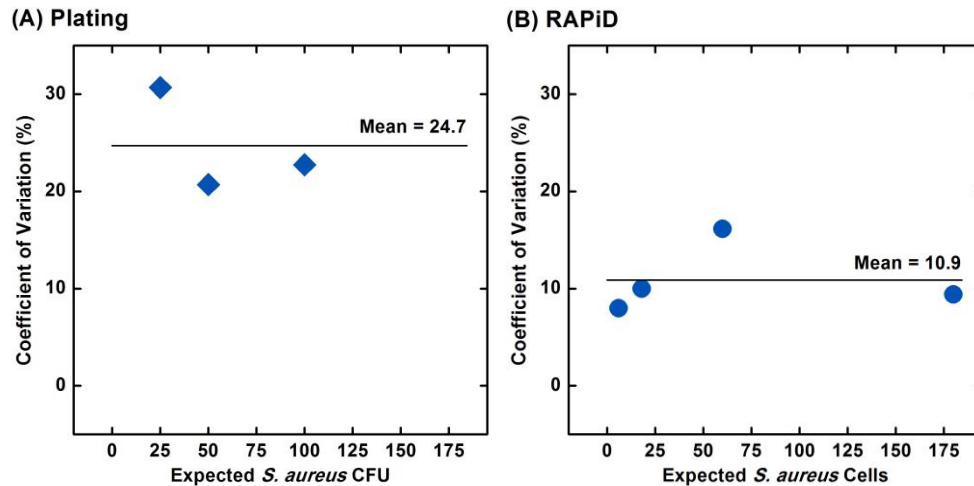


Figure S-11. Coefficients of Variation from Plating and RAPiD for *S. aureus*. Coefficients of variation (CV) from enumerating *S. aureus* via (A) plating and (B) RAPiD are calculated by dividing the standard deviations by the means at each expected number of *S. aureus* CFUs (for plating) or cells (for RAPiD). (A) For plating, at the 3 expected numbers of *S. aureus* CFUs, the CVs range from 20.7% to 30.7% and average 24.7% (marked by the horizontal line). (B) In contrast, for RAPiD, at the 4 expected numbers of *S. aureus* cells, the CVs range from 8.0% to 16.1% and average at 10.9% (marked by the horizontal line). The smaller spread in CVs from RAPiD provides strong support that RAPiD offers a more precise method for enumerating *S. aureus*.

Supplementary Videos

Video S-1. Sample Loading in Picoarray. The Picoarray device is vacuumed prior to sample loading. The vacuum established within the device allows the sample (green food dye as mock sample in this video) to autonomously flow through the branch channels within seconds and fill 100% of all picochambers in ~15 s.

Video S-2. Sample Digitization in Picoarray. After the sample (green food dye as mock sample in this video) completely fills picochambers, silicone oil is injected into the Picoarray device. The oil flows through the branch channels to the outlet but not into sample-filled picochambers, thus partitioning each picochamber from its neighbors and achieving 100% sample digitization in ~10 s.